Forsch Ingenieurwes (2021) 85:567–582
https://doi.org/10.1007/s10010-021-00447-0

ORIGINALARBEITEN/ORIGINALS

Influence of running-in operating conditions on the steady-state torque loss of ground spur gears

Carlos M. C. G. Fernandes[1] · João C. Pais[2] · Ramiro C. Martins[2] · Jorge H. O. Seabra[1]

Received: 5 November 2020 / Accepted: 16 February 2021 / Published online: 15 March 2021

Abstract

The influence of gear running-in operating conditions on the steady-state efficiency of ground spur gears is not well established. However, it is accepted that less rough surfaces promote better efficiency.

Five ground spur gears with similar surface finishing were submitted to two distinct test stages: (i) running-in stage and (ii) torque loss stage. During the running-in stage, five different running-in operating conditions were conducted to ascertain the influence of the load and temperature on the subsequent steady-state gear torque loss test.

The mass loss and surface roughness parameters were influenced by the running-in operating conditions. However, different surface conditions after running-in had only a transient effect on the torque loss measured subsequently. So, the test campaign allow to conclude that even after a severe running-in operating condition, the gears surface still evolves in a significant way during the torque loss tests.

Einfluss der Einlaufbetriebsbedingungen auf den stationären Drehmomentverlust von geschliffenen Stirnrädern

Zusammenfassung

Der Einfluss der Einlaufbetriebsbedingungen auf den stationären Wirkungsgrad von geschliffenen Stirnrädern ist nicht genau bekannt. Es wird jedoch angenommen, dass weniger raue Oberflächen einen besseren Wirkungsgrad begünstigen. Fünf geschliffene Stirnräder mit ähnlicher Oberflächenbearbeitung wurden zwei verschiedenen Testphasen unterzogen: (i) Einlaufphase und (ii) Drehmomentverlustphase. Während der Einlaufphase wurden fünf verschiedene Einlaufbetriebsbedingungen durchgeführt, um den Einfluss der Last und der Temperatur auf den anschließenden stationären Drehmomentverlusttest des Zahnrads zu ermitteln. Die Parameter Massenverlust und Oberflächenrauheit wurden durch die Einlaufbetriebsbedingungen beeinflusst. Unterschiedliche Oberflächenzustände nach dem Einlaufen hatten jedoch nur einen vorübergehenden Einfluss auf den anschließend gemessenen Drehmomentverlust. Die Studie lässt also den Schluss zu, dass sich die Zahnradoberfläche auch nach einem schweren Einlaufbetrieb während der Drehmomentverlusttests noch signifikant verändert.

1 Introduction

According to Blau [1], the running-in is "the process which occurs prior to steady-state operation when two or more solid surfaces are brought together under load and moved relative to one another. This process is usually accompanied by changes in macroscopic friction of force and/or rate of wear".

Shortly after the start of sliding contact between fresh and unworn solid surfaces, changes in friction, temperature, and rate of wear occur. While we accept the fluctuations as the normal course of a mechanism operation, the engineers know that the bearings, gears, and seals performance improve if the running-in stage is optimal [2, 3]. When two machined surfaces are in contact, they touch only by the highest peaks, which makes the current contact area lower

✉ Carlos M. C. G. Fernandes
cfernandes@fe.up.pt

[1] FEUP, Universidade do Porto, Rua Dr. Roberto Frias s/n, 4200-465 Porto, Portugal

[2] ISEP, Instituto Politécnico do Porto, R. Dr. António Bernardino de Almeida 431, 4200-072 Porto, Portugal

Table 1 Nomenclature

Quantities		
ΔT_{GB}	Stabilization temperature of the oil	°C
ΔV	Volume worn out	m^3
ϵ_α	Gear contact ratio	
Λ	Specific film thickness	
μ_{mZ}	Average gear coefficient of friction	
ν	Lubricant kinematic viscosity	cSt
$\overline{\Lambda}$	Mean specific film thickness	
$\overline{\mu_{mZ}}$	Average of the averages coefficient of friction	
$\overline{k}$	Mean wear rate	Pa^{-1}
ρ	Lubricant density	$g\,cm^{-3}$
ρ_{steel}	Steel specific weight	$7850\,g\,cm^{-3}$
σ	Composite roughness	μm
b	Gear face width	mm
E_f	Gear friction energy during running-in	J
F_N	Meshing gear normal load	N
F_r	Bearing radial load	N
H	Softer surface hardness	$N\,m^{-2}$
h_0	Central film thickness	μm
H_{VL}	Gear loss factor	
K	Dimensionless wear rate	
m	Mass	mg
m_l	Gear mass loss	mg
m_r	Reference mass	mg
N_L	Pinion number of cycles	
p_0	Maximum Hertz contact presure	GPa
R_a	Aritmetic average roughness	μm
R_k	Core roughness depth	μm
R_q	RMS average roughness	μm
R_{max}	Maximum roughness	μm
R_{pk}	Reduced peak height	μm
R_{vk}	Reduced valley depth	μm
R_z	Mean peak-to-valley height	μm
S	Sliding distance	m
T_{amb}	Temperature of the room	°C
T_{base}	Temperature of the test rig base	°C
T_{in}	Nominal wheel input torque	Nm
T_{oil}	Oil temperature	°C
T_{V0}	Load independent torque loss	Nm
T_{VD}	Seals torque loss	Nm
T_{VL}	Rolling bearings torque loss	Nm
T_{VZ0}	Load independent gears torque loss	Nm
T_{VZP}	Meshing gears torque loss	Nm
T_V	Total torque loss	Nm
Superscripts		
e	Based on experimental measurement	
Subscripts		
1	Begin	
2	End	
p	Pinion	
w	Wheel	
Ki	Load stage	

than the theoretical one. If these surfaces are running-in under load, these small irregularities can disappear and consequently the real contact area increases. In the beginning, wear is severe and rapid but slows down as the area of the contacting surfaces and its specific film thickness increases.

During a running-in process, three discrete phases usually occur according to Jamari [4]. In the first phase, there is usually a significant decrease in the surface roughness and the coefficient of friction. In the second phase, the existing contact results in increased hardness and stresses but no significant modification on the roughness and friction [5]. In the third phase, we achieve steady conditions of the surfaces because it reaches the equilibrium between all the mentioned factors. It is naturally desirable for a machine element to operate in this third stage to extend their lifespan or increase the maintenance intervals [6].

Several efforts have been made in order to depict the influence of surface waviness and roughness on the running-in and wear mechanisms of lubricated contacts [7–12].

Andersson et al. [13] carried out a study comparing super finished and ground gears to verify if greater contact pressure during the running-in phase is beneficial to improve efficiency. The conclusion was that super finished gears did not show significant changes in the roughness parameters after the running-in.

Sjöberg et al. [14] investigated the influence of the load during the running-in phase on the efficiency of the gears. The researchers concluded that a higher load in the running-in phase allows for improving gear efficiency. In terms of surface roughness, they observed that the greater the load during running-in the greater the effect on the surface roughness.

Sosa et al. [15] used a mechanism that allowed them to study the phenomenon of running-in without disassembling the gear, using equipment to measure roughness and power loss during the entire process. They observed the changes in the surfaces during the running-in period and concluded that the changes in the surface occur in the initial cycles of operation (between 40 and 50 initial cycles). At the beginning of the test, there was a fast drop in the coefficient of friction but a slight increase in the same coefficient of friction during running-in. The authors concluded that different loads

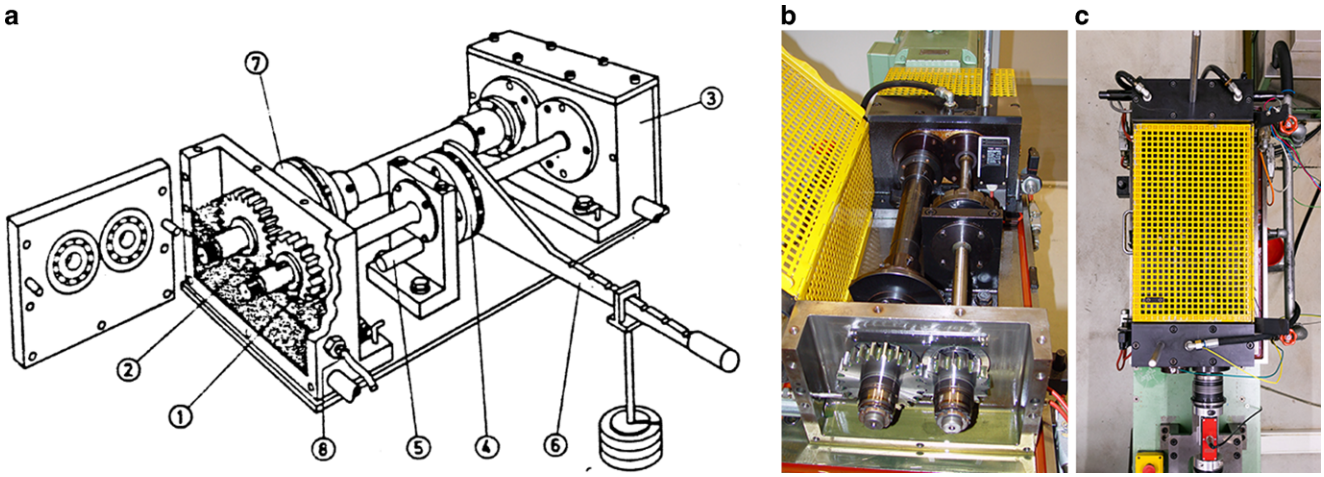

Fig. 1 FZG gear test rig [18]

during running-in changed the gear mesh efficiency over the whole range of velocities tested. In particular, a higher load during running-in promoted a higher efficiency during the power loss tests. The running-in load has a larger effect on meshing efficiency than the operating temperature. The efficiency tests had a duration of 5 min for each operating condition studied.

Mallipeddi et al. [16] studied the effect of the load on the evolution of the surface characteristics of the gears and subsequently performed efficiency tests. The authors concluded that the running-in phase and the efficiency tests changed the surface roughness in a layer smaller than 10 μm on average. The researchers also concluded that a higher load during the running-in phase and during the efficiency tests promoted a bigger chance of micro-pitting occurrence because of the surface irregularities and the stress concentrations. Mallipeddi et al. [16] observed that plastic deformation zones appear after the efficiency tests with a dimension lower than 5 μm and no cracks grow on those zones.

The aim of this work is to study the influence of load and oil temperature during running-in, and how this affects the steady-state gear torque loss. Gear tests are developed in two different stages: (i) running-in and (ii) torque loss. The first stage is called (i) running-in and all the gears (G1 to G5) were submitted to different operating conditions for 8 hours. Then, all the gears were submitted to a (ii) torque loss test campaign (using the same operating conditions and duration) to verify the influence of the running-in conditions on the torque loss results obtained. The evolution of gear tooth flanks is analysed at the end of each stage, comparing surface roughness, gear mass loss (wear) and torque loss.

2 Test rig, gear geometries and lubricant

2.1 FZG Test rig

Fig. 1 shows the FZG gear test rig. This machine operates with a recirculating power loop principle to provide a constant torque load to a pair of test gears. Two torsional shafts connect the driving gearbox (3) and the test gearbox.

The shaft connected to the test pinion (1) has a load clutch to apply a fixed torque by putting up known weights

Table 2 Technical specifications of the ETH DRDL II torque cell

Torque transducer type DRDL II	
Nominal torque / Nm	50
Measurement range / Nm	10/50
Non-linearity / %	< 0.1
Hysteresis / %	< 0.1
Accuracy / %	0.01
Temperature sensitivity / % K^{-1}	0.01
Torque measuring module type ValuemasterBase	
Accuracy / %	0.02
Non-linearity / %	0.1

Table 3 Geometry of the gears (C14, b = 14 mm) and (C40, b = 40 mm)

Parameter	Pinion	Wheel
Number of teeth	16	24
Module / mm	4.5	
Axis distance / mm	91.5	
Pressure angle / °	20	
Profile shift	0.1817	0.1715
Tip diameter / mm	82.64	118.54
Contact ratio ε_α	1.44	
Material	20MnCr5	
Treatment	Case hardened	

Table 4 PAO ISO VG 150 gear oil properties

Kinematic viscosity, ν @ 40 °C / cSt	151.96
Kinematic viscosity, ν @ 70 °C / cSt	46.51
Kinematic viscosity, ν @ 100 °C / cSt	18.89
Density, ρ @ 15 °C / g cm^{-3}	0.854
Pour point / °C	< −57
Flash point / °C	250

to the loading arm. A load clutch divides this shaft into two parts and uses the locking pin (5) to fix one part of the load clutch. Then, the loading lever (6) and weights allow the twisting of the other part.

An ETH Messtechnik DRDL II torque transducer assembled on the FZG test machine allowed to measure the torque loss, as shown in Fig. 1c. The technical characteristics of the sensor are displayed in Table 2 [17]. The system uses a sensor interface (ValuemasterBase) to communicate with a PC with an Ethernet connection. Integrating the torque cell with the software allows recording the torque loss values with an adjustable sampling rate (from 1 Hz to 1000 Hz).

2.2 Gear geometries and lubricant

The driving gearbox (3) operated with type C40 gears under oil jet lubrication [18]. The oil pressure of the lubrication system was 0.35 bar to assure a flow rate of 31 min^{-1}.

The test gearbox operated with type C14 gears under 1.5 l oil dip lubrication. Table 3 lists the main properties of each gear type geometry. The gears are standard FZG gears supplied by ZF.

Both the test and the driving gearboxes were lubricated with an ISO VG 150 fully formulated gear oil that complies with the DIN 51517 part 3 (CLP). The lubricant has a poly-α-olefin (PAO) base oil and presents the physical properties listed in Table 4.

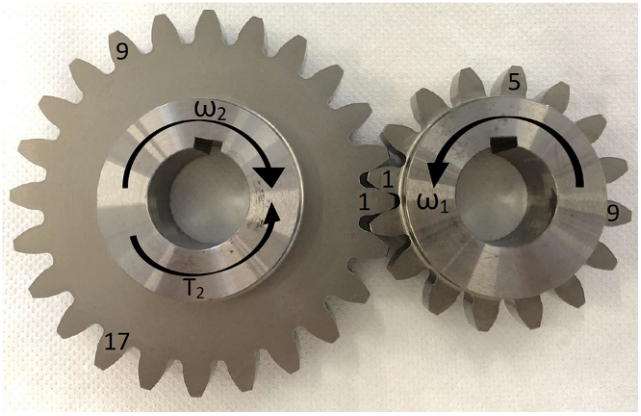

Fig. 3 Surface roughness measurement position

3 Test campaign

The test campaign follows the scheme presented in Fig. 2.

3.1 Pre and post test analysis

Before any measuring procedure of the test campaign (mass, roughness, running-in or power loss) the gears are cleaned in a ultrasound bath with petroleum ether for 5 min.

The gear surface roughness measurements were done using a Hommelwerke T8000 controller. A TK300 pickup

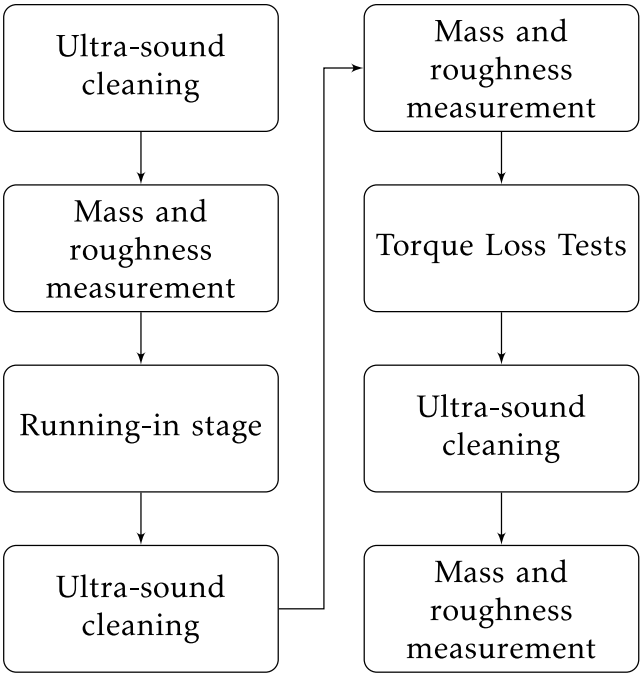

Fig. 2 Test campaign sequence

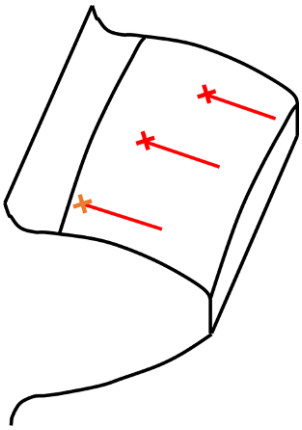

Fig. 4 Surface roughness measurement location in each tooth

with a vertical range of measurement of $\pm 300\,\mu$m, a tip radius of $5\,\mu$m and a cone angle of 90° was used.

Fig. 3 defines the teeth selected for surface roughness measurement, the rotating direction, and the wheel nominal torque. The surface roughness measurements were performed in radial direction before and after each test in teeth numbers one, five and nine of the pinion and in teeth numbers one, nine and seventeen of the wheel, according to Fig. 4. The tooth numbering allow to monitor the surfaces that contact with each other. In the beginning of each test, it is assured that tooth one from the pinion is assembled in contact with tooth one from the wheel.

The roughness parameters were measured according to the standards DIN4762, DIN4768 and DIN4776 [19]. A traversing length of 4.8 mm and a cut-off length of 0.8 mm were selected.

The mass of the pinion and wheel was measured with a scale with ± 1 mg precision. A reference pinion with mass m_r was also measured in each time to depict scale calibration issues. The mass loss is then calculated according to Eq. (1).

$$m_l = (m_2 - m_1) + (m_{r_2} - m_{r_1}) \tag{1}$$

4 Models and equations

4.1 Specific film thickness

The specific film thickness Λ was calculated with the Talian's equation (2) [20]. The central film thickness h_0 was calculated according to Grubin formula, given by Dowson and Higginson [21], at the pitch point. The composite surface roughness σ was evaluated using Eq. (3). The mean R_q values are in Tables 12 and 13 for the pinion and wheel, respectively.

$$\Lambda = \frac{h_0}{\sigma} \tag{2}$$

$$\sigma = \sqrt{Rq_p{}^2 + Rq_w{}^2} \tag{3}$$

4.2 Wear rate

Archard [22] proposed a wear law that describes the wear volume loss due to the sliding contact between flat surfaces according to Eq. (4):

$$\Delta V = \frac{K}{H} \cdot F_N \cdot S \tag{4}$$

K is the dimensionless wear rate, H is the softer surface hardness, F_N is the meshing gear normal load and S is the sliding distance. In the present case, the worn volume ΔV is calculated according to Eq. (5) using the mass loss m_l for steel gears with a material density ρ_{steel}.

$$\Delta V = \frac{m_l \times 10^{-6}}{\rho_{steel}} \tag{5}$$

Brandão et al. [23] derived a mean wear rate $\overline{k}$ using the mass loss for the gears tested according to Eq. (6) where N_L is the pinion number of cycles.

$$\overline{k} = 3.140 \times 10^{-9} \cdot \frac{m_l}{N_L \cdot F_N} \tag{6}$$

4.3 Coefficient of friction derived from torque loss tests

In early works [17] the authors presented the torque loss in an FZG test rig with driving and test gearboxes assembled with C40 gears [18, 24–28]. The results allowed the calibration of a power loss model.

Taking into account the average of all K1 load stage measurements collected in the present study, $\overline{T^e_{V_{K1}}}$, it is possible to calculate the no-load gear T_{VZ0} and seal torque T_{VD} losses according to Eq. (7) [24].

$$T_{V0} = T_{VZ0} + T_{VD} = \overline{T^e_{V_{K1}}} - T_{VL} \tag{7}$$

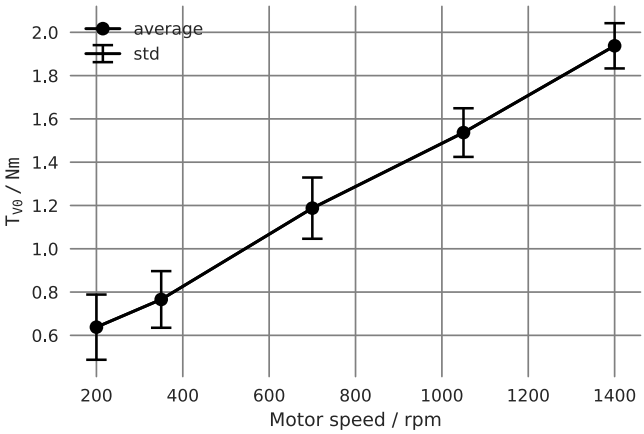

Fig. 5 No-load torque loss

Table 5 No-load losses

Speed / rpm	T_{V0} / Nm	SD / Nm
200	0.57	0.15
350	0.67	0.13
700	1.04	0.14
1050	1.32	0.11
1400	1.65	0.10
1850	2.75	0.48

Table 6 SKF model coefficients determined experimentally

Test	Running-in	After Running-in
μ_{bl}	0.0409	0.0326
μ_{EHL}	0.0155	0.0154

T_{VL} are the bearing losses. Fig. 5 shows the no-load losses T_{V0} of the FZG test rig based on the K1 load stage measurements according to Eq. (7). The standard deviation is also presented. The results show that an increasing speed results in higher no load losses, as expected. The maximum standard deviation of the no-load losses calculation presented in Table 5 is considered as a measure of the accuracy of the meshing torque loss $T^e_{VZP_{Ki}}$ prediction (Eq. 8). The differences between the gears tested (G1 up to G5) that are below ±0.15 Nm have no practical meaning. The values measured for the operating speed of 1850 rpm in the wheel were disregarded because there is an unexpected difference on the measured K1 total torque loss among the different gears whose reason needs further study.

The rolling bearings torque loss T_{VL} were predicted using the SKF model [29]. The calibration of the model considers the influence of the lubricant after rolling bearing tests lubricated with the PAO ISO VG 150 gear oil [18]. Table 6 presents the model coefficients determined for two distinct bearing conditions: during and after running-in phase.

To calculate the friction torque loss generated by the meshing gears equation (8) is used.

$$T^e_{VZP_{Ki}} = T^e_{V_{Ki}} - (T_{V0} + T_{VL_{Ki}}) \tag{8}$$

If the meshing gears torque loss $T^e_{VZP_{Ki}}$ is already quantified (Eq. 8), an experimental average coefficient of friction (μ^e_{mZ}) for all gear meshes of the gearbox is possible to estimate. The average coefficient of friction μ^e_{mZ} can be calculated according to Eq. (9) considering that the test-rig operates with 2 meshing gears with the same gear loss factor H_{VL}.

$$\mu^e_{mZ} = \frac{T^e_{VZP}}{2 \cdot T_{\text{in}} \cdot H_{VL}} \tag{9}$$

4.4 Friction Energy

The friction energy E_{f} during running-in can be calculated using Eq. (10).

$$E_{\text{f}} = P_{\text{in}} \cdot H_{VL} \cdot \int_{t_1}^{t_2} \mu^e_{mZ}(t)\, dt \tag{10}$$

P_{in} is the input power, H_{VL} is the gear loss factor, t_1 and t_2 are respectively the begin and end time.

A mean average coefficient of friction $\overline{\mu_{mZ}}$ can also be calculated using Eq. (11).

$$\overline{\mu_{mZ}} = \frac{\int_{t_1}^{t_2} \mu_{mZ}(t)\, dt}{t_2 - t_1} \tag{11}$$

5 Running-in phase

5.1 Operating conditions

The running-in tests were performed under different load and temperature conditions to test their influence on surface roughness, mass loss, and torque loss. Each running-in stage used a new gear flank. These gears are different only in the surface finishing, despite being very similar, are not equal. It is almost impossible to achieve equal surface finishing in two ground gears.

The operating conditions used during the running-in tests are presented in Table 7. The parameters of interest for the running-in were the oil operating temperature and the gear nominal load (torque applied to the pinion). The running-in tests were all run at 200 rpm (wheel speed), assuring a low specific film thickness ($\Lambda < 0.1$). Each running-in phase lasts 8 hours corresponding to 144 000 cycles of the pinion.

The torque loss and the operating temperatures (T_{oil}, T_{amb}, T_{base}) were measured continuously during the running-in phase.

During the running-in period, the driving gearbox (C40) operated under oil jet lubrication while the test gearbox (C14) operated under oil bath lubrication, as described in Sect. 2.2.

Table 7 Operating conditions for running-in stage

Gear	Load stage[a]	T_{oil} / °C	Pinion Torque / Nm	p_0^{C40} / GPa[b]	p_0^{C14} / GPa[b]
G1	K9	80	215.6	0.83	1.40
G2	K11	80	319.2	1.01	1.70
G3	K6	90	98.8	0.56	0.95
G4	K9	90	215.6	0.83	1.40
G5	K11	90	319.2	1.01	1.70

[a] load stages with a load lever arm of 0.35 m; [b] p_0 at pitch point

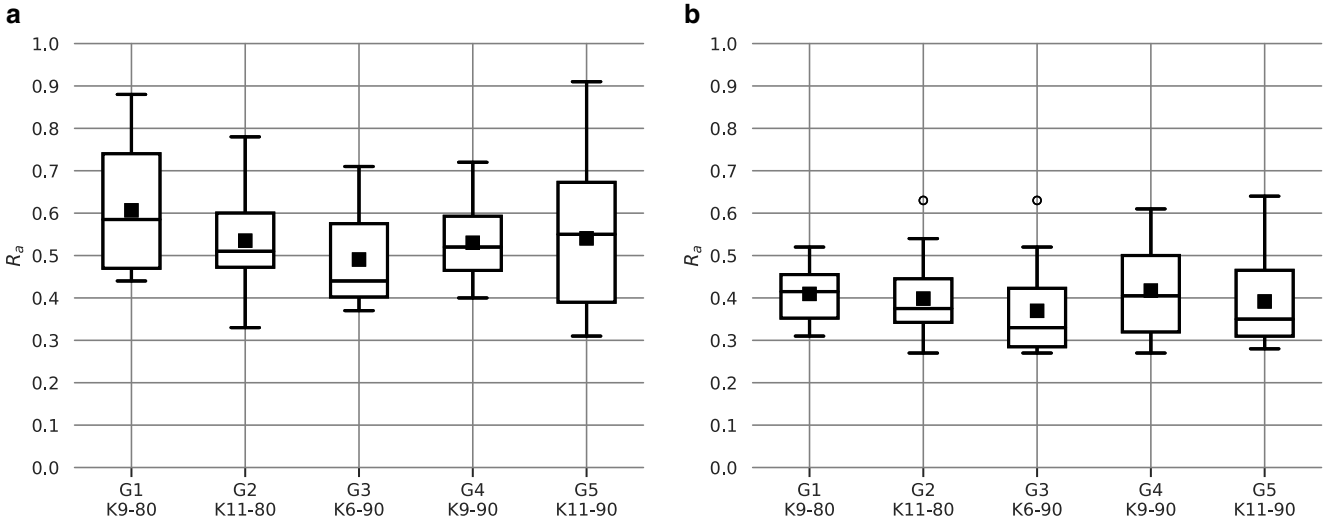

Fig. 6 Arithmetic average roughness R_a of 18 measurements. **a** New gears, **b** gears after running-in phase

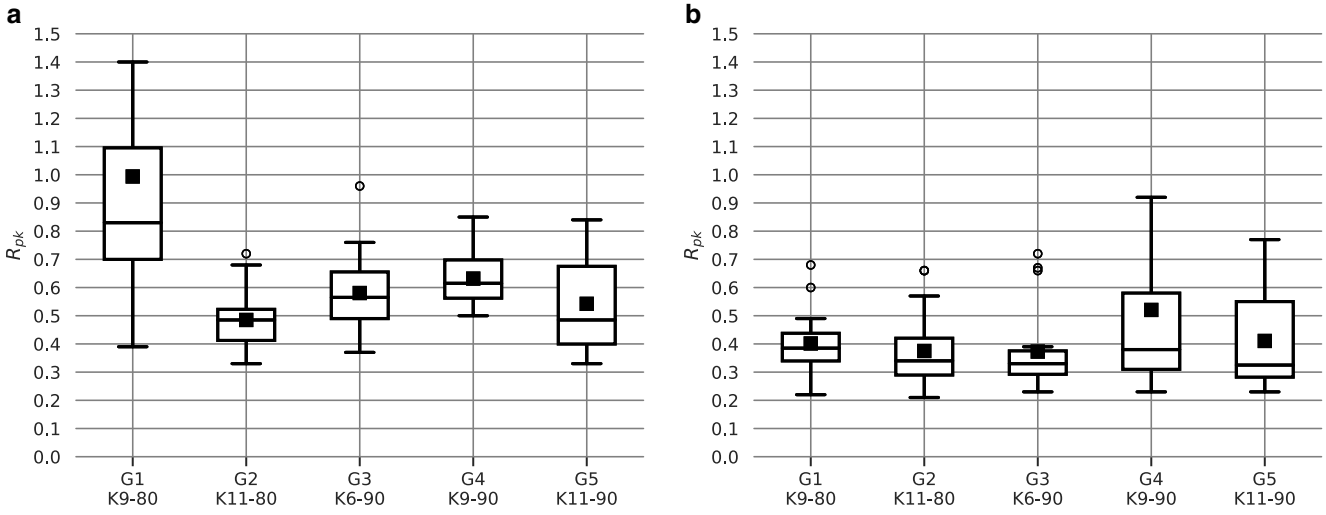

Fig. 7 Reduced peak height R_{pk} of 18 measurements. **a** New gears, **b** gears after running-in phase

5.2 Surface roughness evolution

The surface roughness of the C40 gears tested in the driving gearbox was measured before any test has been performed and the results are resumed in Table 14.

Figs. 6 and 7 present the normal distribution of the 18 measurements of the R_a and R_{pk}, respectively, and present two distinct results: new gears and gears after running-in phase.

All the figures present the median (line) and the mean value (point). The sample is skewed because the wheel surface usually presents lower roughness parameters than the pinion after the manufacturing process. For skewed samples, the median is usually better than the mean value for the trend of the set [30]. The new gears tend to present a positively skewed distribution as observed in Fig. 6a and Fig. 7a. However, the values of R_a and R_{pk} of the five gears, after the running-in phase, tend to be similar.

Before testing, all the gears presented a similar but not equal median value of R_a. A Kruskal-Wallis H-test was done to test the null hypothesis that the population median of all of the groups are equal. It is a non-parametric version of ANOVA [31]. This is mandatory to exclude automatically a considerable influence of the initial roughness parameters on the subsequent analysis. For the new gears there were no statistically significant differences between group medians of R_a ($p = 0.167$). However, for the new gears there were statistically significant differences between group medians of R_{pk} ($p = 5.149 \times 10^{-6}$). In particular the gear G1 presented higher median value of R_{pk} than other gears. A detailed analysis of the Abbott-Firestone curves allowed to verify that 2 profiles out of 18 measurements

were causing a larger mean and median value of R_{pk} for the gear G1 (new condition).

After the running-in there were no statistically significant differences between group medians of R_a ($p = 0.415$) and R_{pk} ($p = 0.502$). These results indicate that during running-in phase the surface roughness of the teeth flanks suffer considerable modifications and reduction of the R_a and R_{pk} roughness parameters.

While the median values are not efficient in depicting which operating condition decreases R_a in a considerable way, the interquartile size among groups is smaller after running-in phase. The smaller interquartile range is observed for the tests at 80 °C independently of the nominal load, i.e. the dispersion of measurements is lower. The evolution of R_{pk} is remarkable for the running-in phase at 80 °C. Such results allow to conclude that a slightly higher specific film thickness (80 °C) promoted a fast variation on the reduced peak height. The higher wear observed at 90 °C promoted a similar variation of R_a in comparison with 80 °C but a smaller variation on the R_{pk}.

The running-in tests performed at 80 °C presented a smaller variance on the R_a and R_{pk} among 18 measurements in each gear tested. The mean value of R_{pk} is lower for 80 °C but the median value is similar to 90 °C.

5.3 Specific film thickness

Fig. 8 presents the specific film thickness calculated for the beginning and the end of each gear running-in phase. The surface roughness evolves during the running-in phase, and an evolution on the specific film thickness is also expected. The specific film thickness increased during all the running-in operating conditions tested. The increment of the specific film thickness for the gears tested at 90 °C was smaller than for the gears tested at 80 °C or low load (K6).

These results suggest that the specific film thickness is mandatory in the R_{pk} achieved after running-in. However, R_a was not influenced by a slightly different specific film thickness.

5.4 Mass loss

Fig. 9 and Table 8 present the mass loss after running-in both for the pinion and the wheel.

The gears tested under load stage K11 (G2 and G5) had a significantly lower mass loss than the gears tested in load stages 6 (G3) and 9 (G1 and G4); indicating that the wear mechanisms in gears G2 and G5 are different from the wear mechanisms that occurred in the other gears.

The experimental results show that a higher operating temperature generated higher mass loss, which might indicate that the gears tested at 90 °C achieved a more developed phase of the running-in process. The mass loss measurements are done in the milligram range, so it is difficult to

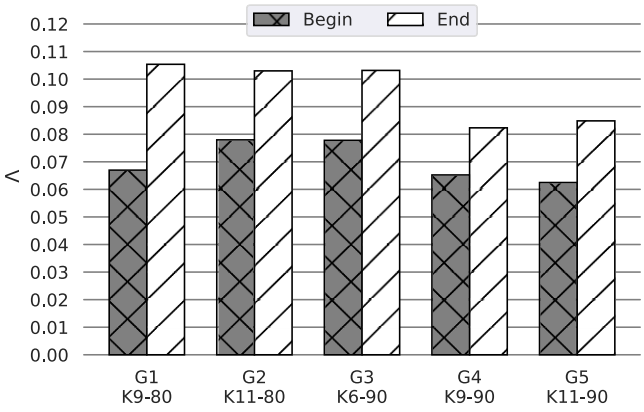

Fig. 8 Specific film thickness at the begin and end of running-in phase (at the pitch point)

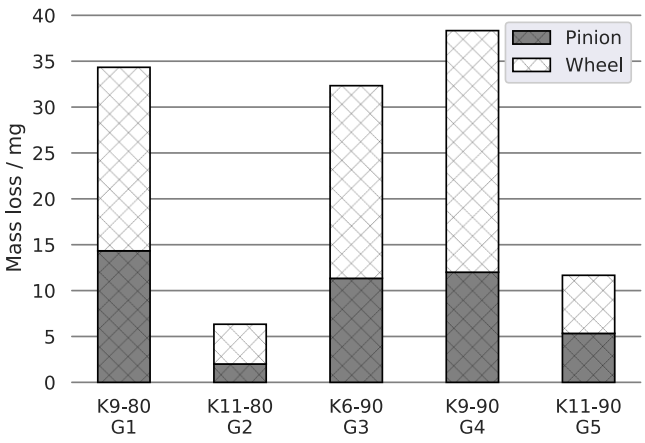

Fig. 9 Mass loss after running-in phase

Table 8 Mass loss after running-in phase [mg]

Gear	Run-in Condition	Pinion	Wheel	Total
G1	K9-80	14	20	34
G2	K11-80	2	4	6
G3	K6-90	11	21	32
G4	K9-90	12	26	38
G5	K11-90	5	6	11

get clear trends between the operating conditions and mass loss measurements in short time duration tests. In the case of gears G1 and G4, the differences are particularly small. Despite the small differences observed, the trend for gear (pinion + gear) was observed both for G1 vs G4 and G2 vs G5, i.e. higher operating temperature increased mass loss.

The mass loss results when crossed with the surface roughness measurements show that a larger specific film thickness on the running-in phase is beneficial for the reduction of R_{pk}. The gear G3 which operated under a lower load (K6) and a higher temperature (90 °C), besides the similar specific film thickness in comparison with both G1 and G2, presented the lowest variance on the R_a and R_{pk}.

Overall, comparing similar loading conditions, the differences in the mass loss measurements are very small. Furthermore, the repeatability of the mass loss measurements was not verified in the present work.

5.5 Wear rate

Fig. 10 shows the mean wear rate of the tested gears during the running-in tests. The results are presented as function of the estimated specific film thickness (the mean of begin and end of running-in phase values) already presented in Fig. 8. For the same operating load, the mean wear rate is lower for an higher mean specific film thickness. For the same operating temperature, an increasing load promoted a decreasing mean wear rate and eventually a modification on the wear mechanisms.

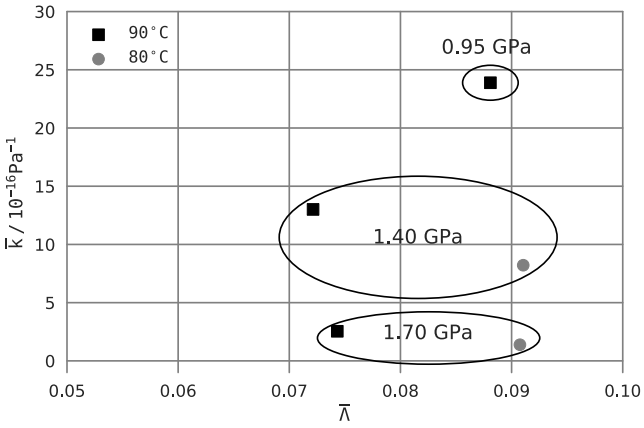

Fig. 10 Mean wear rate vs. specific film thickness during running-in phase

Table 9 Friction energy during running-in

Gear	Running-in	E_f / J	$\overline{\mu_{mZ}}$
G1	K9-80	1847931	0.0519
G2	K11-80	2979072	0.0565
G3	K6-90	575330	0.0352
G4	K9-90	1456475	0.0409
G5	K11-90	2546546	0.0483

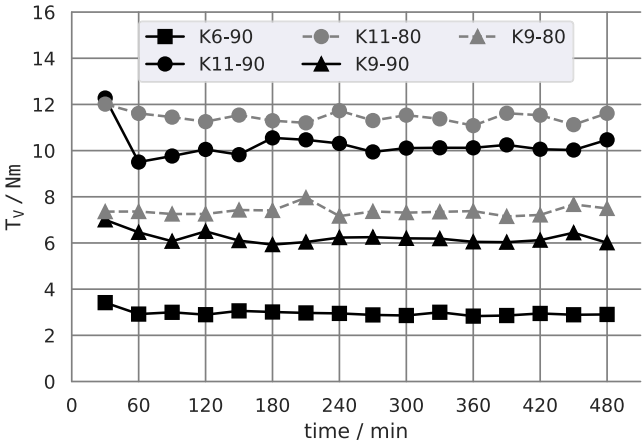

Fig. 11 Total torque loss measurement during running-in phase

However, the mean wear rate calculation is more reliable if steady state wear is occurring, which is not the case during the running-in phase.

5.6 Torque loss

Fig. 11 presents the total torque loss measured during the running-in phase. After 30 min of running-in phase, the average torque loss for the tests operated under the same nominal torque are quite similar. Because different operating temperatures were used (80 or 90 °C), a small difference in the torque loss is expected because both the specific film thickness and the no-load losses due to the oil churning are slightly different.

At 90 °C the torque loss decreased in the subsequent measurements (> 30 min). The tests at 90 °C which present a decrease on the torque loss measured from 30 min to 60 min presented also an higher wear rate. Such behavior is in part explained with a smaller specific film thickness at 90 °C that promoted a higher mean wear rate as presented in Fig. 10. On the other side, such variation is not found for the tests at 80 °C which operated with an higher specific film thickness since the beginning of the running-in phase.

The torque loss results which are a direct indication of the contact friction suggests that the surfaces evolve in a faster way under a smaller specific film thickness which is beneficial for the coefficient of friction.

5.7 Coefficient of friction and friction energy

An average coefficient of friction was calculated for each 30 minute torque loss measurement during running-in using Eq. (9). The results are presented in Fig. 12. The results follow the same trend of the torque loss measurements already discussed.

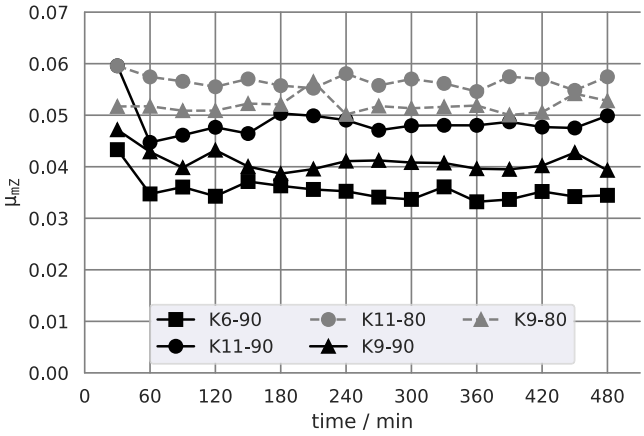

Fig. 12 Average gear coefficient of friction during running-in phase

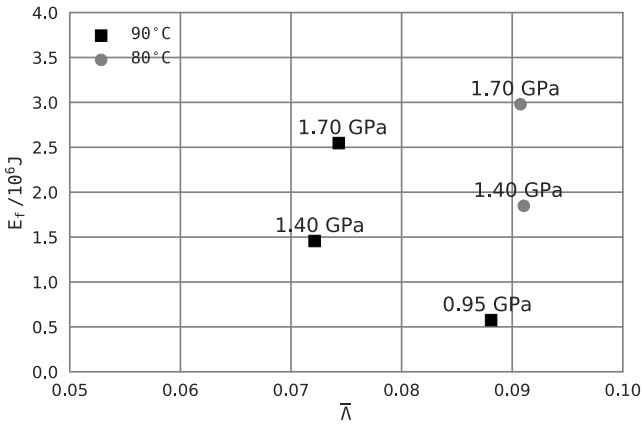

Fig. 13 Friction energy during running-in phase

Table 9 presents the friction energy calculted with Eq. (10) where t_1 = 1800 s and t_2 = 28 800 s. The mean value of the average coefficient of friction during running-in is also presented.

Fig. 13 shows that for the same load, a larger friction energy occurs for the gears that reached an higher mean specific film thickness during running-in.

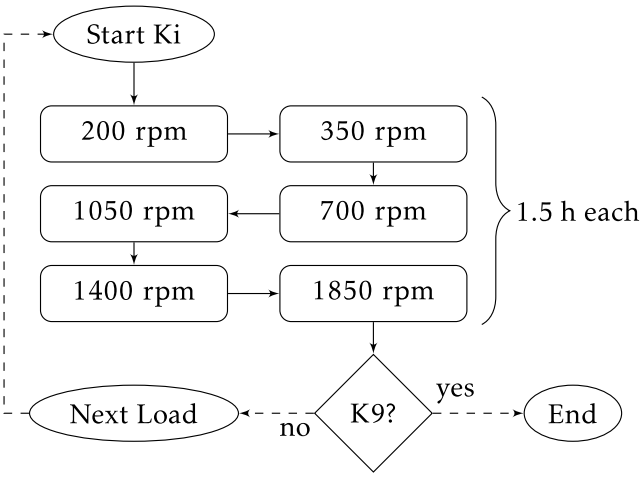

Fig. 14 Torque loss tests sequence

6 Torque loss tests

6.1 Operating conditions

The torque loss tests consisted of heating and controlling the oil temperature in both the FZG gearboxes at 80 °C, and test the gears for 1.5 h with the load stages K1, K5, K7 and K9 at motor speeds of 200, 350, 700, 1050, 1400, 1850 rpm, which correspond to the tangential speeds of 1.14, 2.0, 4.0, 6.0, 8.0, 10.6 m s^{-1} (Table 10). The torque loss tests sequence is presented in Fig. 14.

During the torque loss tests, the driving gearbox (C40) operated under oil jet lubrication while the test gearbox (C14) operated under oil bath lubrication, as described in Sect. 2.2. Both the test and the driving gearbox lubricant temperature were 80 °C. A system composed of resistors incorporated in the test gearbox heats the oil bath. The oil jet lubrication system operated continuously overnight to keep the temperature constant in the reservoir and to stabilize the temperatures of the entire test rig.

The values presented for torque loss and temperature are the average value of the last 30 min of operation. The procedure takes into account only the steady-state operating conditions. Usually, under imposed oil temperature the test-rig reaches thermal equilibrium after 45 min of operation if the oil jet lubrication system operates continuously overnight [17].

Table 10 Operating conditions for the torque loss tests [18]

Load stage[a]	Pinion Torque / Nm	F_N / N	F_r / N	p_0^{C40} / GPa	p_0^{C14} / GPa
K1	3.3	98	49	0.10	0.17
K5	70.0	2069	1034	0.47	0.80
K7	132.5	3915	1958	0.65	1.10
K9	215.5	6371	3185	0.83	1.40

[a] load stages with a load lever arm of 0.35 m

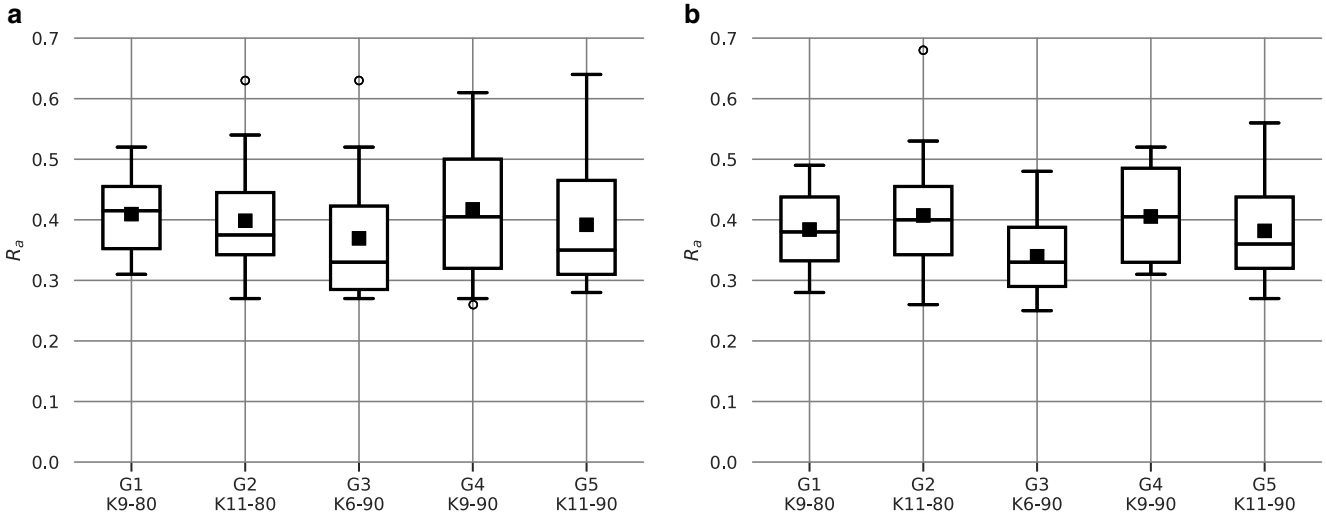

Fig. 15 Arithmetic average roughness R_a of 18 measurements. **a** Gears after running-in phase, **b** gears after torque loss test

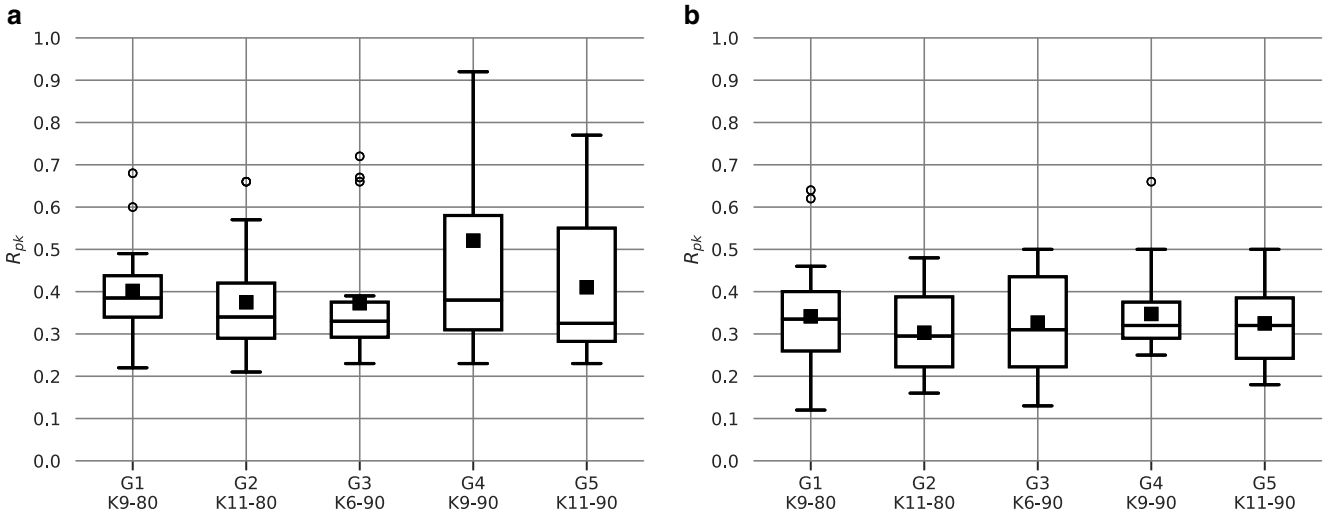

Fig. 16 Reduced peak height R_{pk} of 18 measurements. **a** Gears after running-in phase, **b** gears after torque loss test

6.2 Surface roughness evolution

Figs. 15 and 16 present the normal distribution of the 18 measurements of the R_a and R_{pk}, after running-in and after torque loss tests.

After the torque loss tests, there were no statistically significant differences between group medians R_a ($p = 0.101$) and R_{pk} ($p = 0.841$). However, it is possible to conclude that the gear with running-in phase at K6 and 90 °C (G3) presented a smaller R_a but similar R_{pk} in comparison with the other groups.

After torque loss tests the variance among each group is similar both for R_a and R_{pk}. Such result suggest that a steady surface condition is achieved during the torque loss tests.

6.3 Mass loss

Table 11 presents the mass loss after torque loss tests both for the pinion and the wheel.

The gears that operated during running-in phase with an oil temperature of 80 °C presented a higher mass loss during the torque loss tests.

The results indicate that the gear with running-in performed at K6 and 90 °C promoted the lowest mass loss during the torque loss tests. However, the gear G3 already presented the smaller median R_a before any test.

The mass loss, despite being different among groups, is still very low to be correlated with significant surface roughness evolution during the torque loss tests.

Table 11 Mass loss after torque loss test [mg]

Gear	Run-in Condition	Pinion	Wheel	Total
G1	K9-80	7	11	18
G2	K11-80	7	8	15
G3	K6-90	1	4	5
G4	K9-90	5	7	12
G5	K11-90	3	5	8

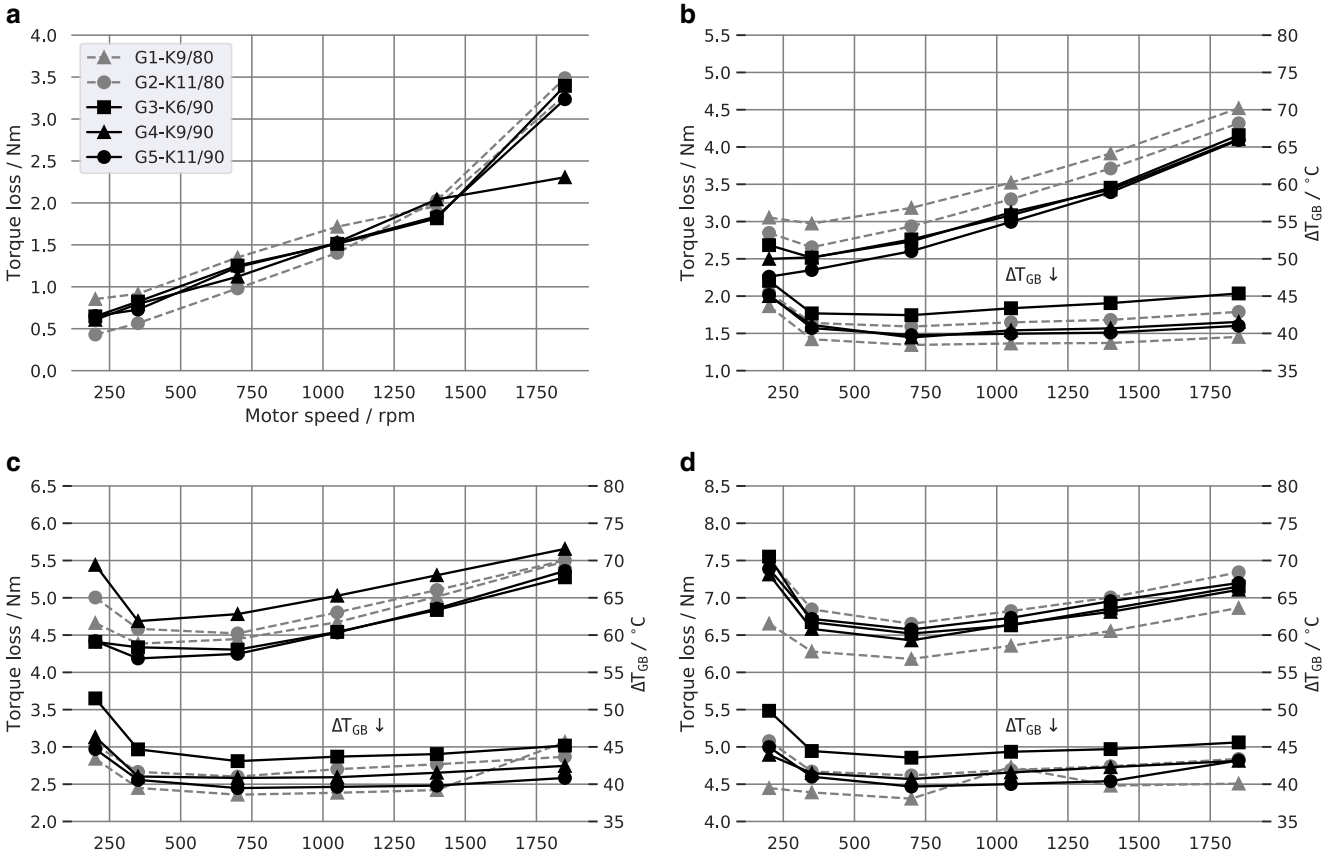

Fig. 17 Torque loss and relative oil temperature ΔT_{GB}. **a** K1, **b** K5, **c** K7, **d** K9

6.4 Torque loss results

After each running-in phase, an efficiency test was performed according to the sequence described in Sect. 6.1. The results are presented in Fig. 17.

The tests performed under K1 load stage allow determining the no-load losses according to the power loss model presented in a previous work [18]. Under K1 load stage is expected to found a very small influence of the surface roughness on the measured torque loss because the meshing gears power loss is negligible as verified in previous works [18, 24]. The experimental results allow to verify that no trend between running-in operating conditions and K1 total torque loss is found.

Fig. 17b shows the total torque loss for a pinion nominal torque of 70 Nm. The gears G1 and G2, with running-in phase at 80 °C, presented higher torque loss than gears G3, G4 and G5 with running-in phase at 90 °C. The gears G1 and G2 presented slightly higher R_a after running-in which can explain a higher torque loss value at K5 load stage.

The total torque loss for the load stage K7 is presented in Fig. 17c. The gears G1 and G2, with running-in at 80 °C, still present higher torque loss than G3 (K6-90) and G5 (K11-90). The differences between the gears tested (G1 up to G5) that are below ±0.15 Nm have no practical meaning as already stated in Sect. 4.3.

Fig. 17d shows the torque loss results for the load stage K9. No significant differences were observed among the gears tested. However, the gear G1, with running-in phase at K9 and 80 °C, presented the lowest torque loss. The difference is within the uncertainty of the measurement as already discussed.

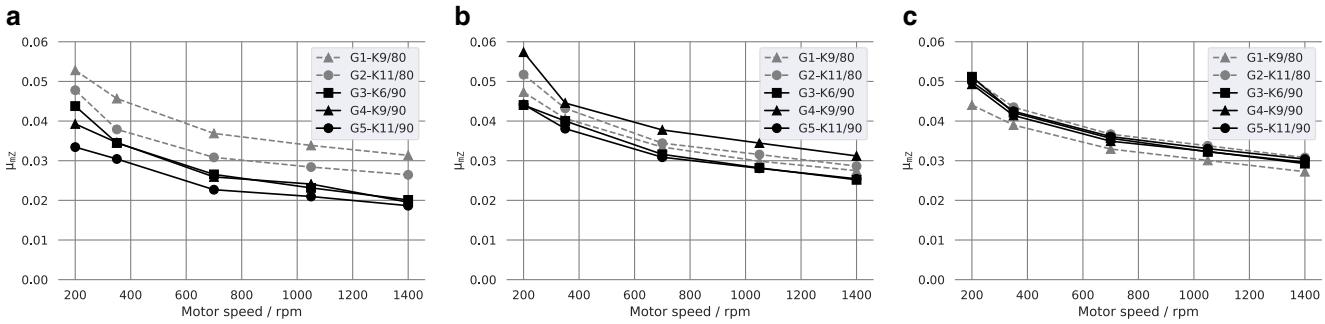

Fig. 18 Coefficient of friction for torque loss tests. **a** K5, **b** K7, **c** K9

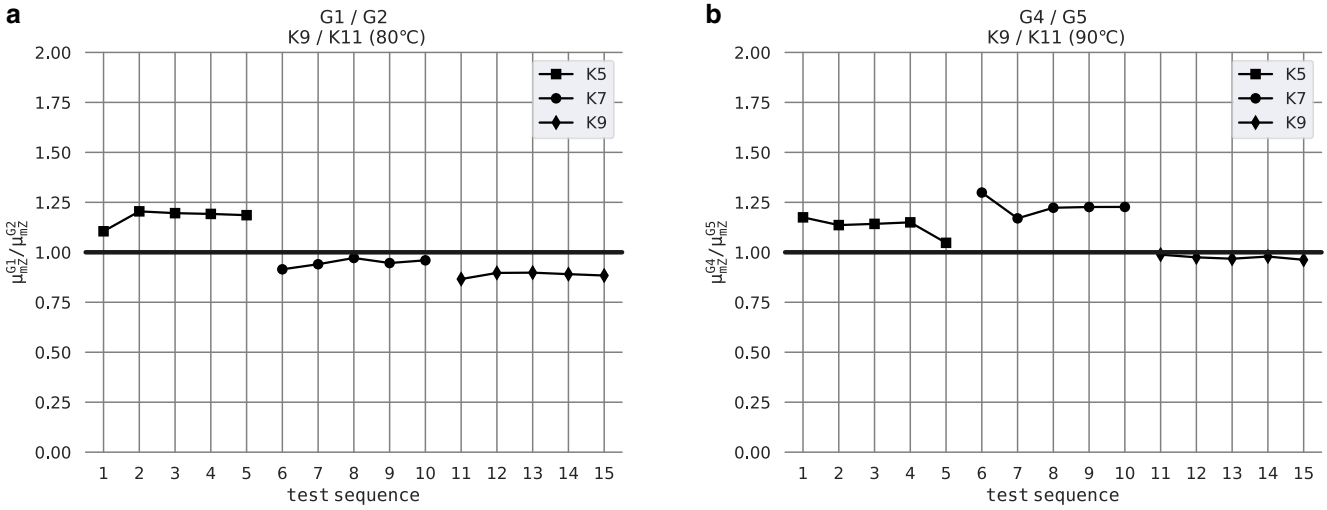

Fig. 19 Influence of the running-in load on the coefficient of friction. **a** K9 vs. K11 (80 °C), **b** K9 vs. K11 (90 °C)

The stabilization temperature of the gearbox ΔT_{GB} can be estimated according to Eq. (12) [32]. The authors that developed the equation found that the relative oil temperature of the FZG gearbox presents the same trend of the torque loss measurements. The ambient T_{amb}, oil T_{oil} and also the base test rig temperature T_{base} are taken into account.

$$\Delta T_{GB} = T_{oil} - \frac{T_{amb} + T_{base}}{2} \tag{12}$$

Fig. 17 shows the oil relative temperature and the results follow well the torque loss experiments. The oil relative temperature values are not ranked in the same fashion as the torque loss results. This fact can be explained by the different humidity and air conditions found on the laboratory that need further analysis in order to check if those factors play an important role in the torque loss measurements of the present study.

6.5 Coefficient of friction

Fig. 18 shows the average coefficient of friction calculated with Eqs. (8) and (9).

The confidence interval for the meshing gears torque loss is within the standard deviation of the no-load losses (±0.15 Nm).

The meshing gears torque loss and the coefficient of friction for the gears G1 and G2, submitted to a running-in phase under 80 °C, are higher for the K5 load stage. Throughout the efficiency test the coefficient of friction of those gears tends to decrease and at K9 no significant difference is achieved between gears (G1 up to G5).

At K9 load stage the differences among gears are not significant and inside the confidence level of the prediction. So, the authors conclude that with the methods used, at the end of the torque loss tests there were no significant differences on the coefficient of friction of the gears G1 up to G5 submitted to different running-in conditions.

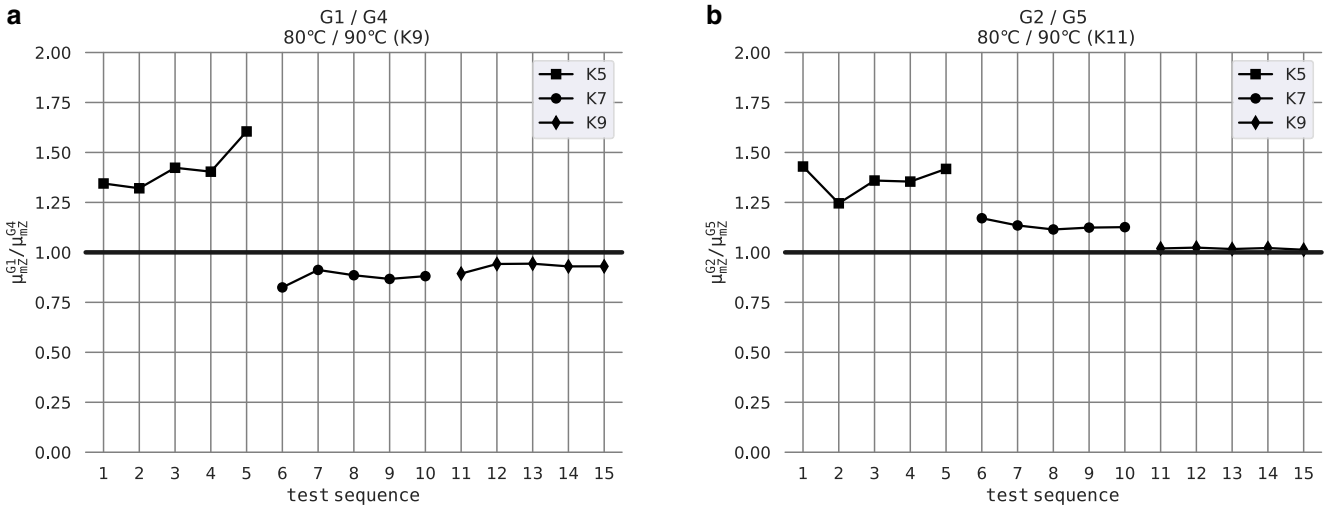

Fig. 20 Influence of the running-in temperature on the coefficient of friction **a** K9 – 80 vs. K9 – 90, **b** K11 – 80 vs. K11 – 90

7 Discussion

7.1 Influence of the running-in load

In order to study the influence of the running-in phase load, a ratio between the coefficient of friction is presented in Fig. 19 keeping the testing sequence. Fig. 19a compares the coefficient of friction ratio of gears G1 and G2 throughout the torque loss tests. Fig. 19b compares the coefficient of friction ratio of gears G4 and G5 throughout the torque loss tests.

In spite of the coefficient of friction being globally smaller during the torque loss tests for the gears with a running-in phase under higher load K11, this is only true during load stages K5 and K7. At K9 load stage, the differences are negligible, no matter the operating temperature considered. Immediately after K9 load stage the gear surface roughness was measured and the differences are also negligible. Such behavior supports the idea that the gears are still running-in during the torque loss tests.

Previous works concluded that the running-in operating conditions have a clear effect on the gear's efficiency. The present study observed the same behaviour for the torque loss tests performed immediately after running-in phase. However, after several hours ($\approx$ 18 h) of torque loss tests (after K5 and K7) the differences observed are negligible both on the surface roughness as well as on the coefficient of friction.

7.2 Influence of running-in temperature (or viscosity)

Fig. 20 presents the influence of the operating temperature on the ratio of the coefficient of friction keeping the testing sequence. Fig. 20a compares the coefficient of friction ratio of gears G1 and G4 throughout the torque loss tests. Fig. 20b compares the coefficient of friction ratio of gears G2 and G5 throughout the torque loss tests.

The coefficient of friction is higher during the torque loss tests for the gears with a running-in phase under lower operating temperature (80 °C). This behaviour was only observed during load stages K5 and K7. After several hours ($\approx$ 18 h) of torque loss tests (after K5 and K7) the differences are negligible, no matter the operating temperature considered.

8 Conclusion

The results presented in this article allow to conclude that:

- A higher operating temperature during running-in phase promoted a smaller specific film thickness and consequently a higher mean wear rate. However, the repeatability of the mass loss measurements needs to be verified in a future work;
- A lower operating temperature during running-in phase promoted an higher coefficient of friction just at the beginning of the torque loss tests;
- The surface roughness parameters keep changing considerably during the torque loss tests which means that the running-in phase was not completely finished after 8 hours;
- The influence of operating conditions during 8 hours of running-in stage is almost negligible on the steady state total torque loss.

Appendix

Roughness Results

Table 12 presents the mean value of 9 measurements on the C14 pinions tested.

Table 13 presents the mean value of 9 measurements on the C14 wheels tested.

Table 14 presents the mean value of 9 measurements on the C40 pinion and wheel tested.

Table 12 Pinion roughness parameters [μm]

Stage	R_a	R_q	R_z	R_{max}	R_{pk}	R_k	R_{vk}
New	0.57	0.72	3.76	4.37	0.56	1.87	0.85
K6-90	0.45	0.57	2.88	3.48	0.45	1.41	0.76
PL	0.40	0.50	2.66	3.36	0.40	1.27	0.68
New	0.67	0.82	3.75	4.45	0.62	2.20	0.92
K11-90	0.48	0.61	2.82	3.47	0.55	1.51	0.73
PL	0.47	0.59	2.81	3.63	0.47	1.44	0.77
New	0.63	0.79	3.76	4.51	0.51	2.04	0.97
K11-80	0.46	0.59	2.86	3.70	0.44	1.52	0.78
PL	0.48	0.62	3.03	3.99	0.38	1.62	0.86
New	0.59	0.75	3.91	4.79	0.67	1.84	0.97
K9-90	0.51	0.69	3.66	5.29	0.72	1.64	0.97
PL	0.48	0.60	3.13	3.72	0.39	1.55	0.89
New	0.68	0.86	4.37	5.15	0.86	2.15	0.89
K9-80	0.47	0.58	2.92	3.40	0.46	1.43	0.76
PL	0.44	0.56	2.87	3.54	0.41	1.31	0.82

Table 13 Wheel roughness parameters [μm]

Stage	R_a	R_q	R_z	R_{max}	R_{pk}	R_k	R_{vk}
New	0.41	0.52	2.93	3.49	0.60	1.32	0.49
K6-90	0.29	0.36	1.93	2.25	0.29	0.89	0.46
PL	0.28	0.36	1.95	2.38	0.25	0.89	0.47
New	0.37	0.47	2.49	2.87	0.43	1.21	0.50
K11-90	0.30	0.38	2.03	2.44	0.27	0.95	0.49
PL	0.31	0.40	2.26	3.03	0.26	0.98	0.61
New	0.44	0.56	3.08	3.60	0.46	1.33	0.74
K11-80	0.33	0.42	2.30	2.90	0.31	0.99	0.64
PL	0.33	0.42	2.37	3.27	0.23	0.96	0.67
New	0.47	0.59	3.13	3.81	0.59	1.56	0.58
K9-90	0.32	0.41	2.15	2.67	0.32	1.00	0.55
PL	0.33	0.43	2.30	2.98	0.30	0.99	0.63
New	0.45	0.58	3.28	3.78	0.54	1.46	0.67
K9-80	0.35	0.43	2.30	2.78	0.34	1.10	0.56
PL	0.33	0.42	2.21	2.74	0.27	1.06	0.56

Table 14 Roughness parameters of C40 gears in radial direction [μm]

	R_a	R_q	R_z	R_{max}	R_{pk}	R_k	R_{vk}
Pinion	0.28	0.39	1.82	2.83	0.37	0.8	0.56
Wheel	0.24	0.32	1.60	2.5	0.23	0.76	0.48

Acknowledgements The authors gratefully acknowledge the funding whom without this work would not have been possible:

- LAETA under the project UID/50022/2020.

References

1. Blau PJ, Komanduri R (1990) Friction and wear transitions of materials: break-in, run-in, and wear-in. J Eng Mater Technol 112(2):254. https://doi.org/10.1115/1.2903318
2. Blau PJ (2005) On the nature of running-in. Tribol Int 38(11-12):1007–1012. https://doi.org/10.1016/j.triboint.2005.07.020
3. Akbarzadeh S, Khonsari M (2011) Experimental and theoretical investigation of running-in. Tribol Int 44(2):92–100. https://doi.org/10.1016/j.triboint.2010.09.006
4. Jamari J (2006) Running-in of rolling contacts, PhD Thesis, University of Twente, Netherlands
5. Andersson S (1977) Initial wear of gears. Tribol Int 10(4):206–210. https://doi.org/10.1016/0301-679X(77)90021-4
6. Chowdhury SR, Kaliszer H, Rowe G (1979) An analysis of changes in surface topography during running-in of plain bearings. Wear 57(2):331–343. https://doi.org/10.1016/0043-1648(79)90107-8
7. Chengwei W, Linqing Z (1991) Effect of waviness and roughness on lubricated wear related to running-in. Wear 147(2):323–334. https://doi.org/10.1016/0043-1648(91)90189-2
8. Shirong G, Gouan C (1999) Fractal prediction models of sliding wear during the running-in process. Wear 231(2):249–255. https://doi.org/10.1016/S0043-1648(99)00132-5
9. Jeng Y-R, Lin Z-W, Shyu S-H (2004) Changes of surface topography during running-in process. J Tribol. https://doi.org/10.1115/1.1759344
10. Akbarzadeh S, Khonsari M (2010) On the prediction of running-in behavior in mixed-lubrication line contact. J Tribol. https://doi.org/10.1115/1.4001622
11. Akbarzadeh S, Khonsari M (2013) On the optimization of running-in operating conditions in applications involving ehl line contact. Wear 303(1):130–137. https://doi.org/10.1016/j.wear.2013.01.098
12. Zhang G, Liu X, Lu W (2013) A parameter prediction model of running-in based on surface topography. Proc Inst Mech Eng H J Eng Med 227(9):1047–1055. https://doi.org/10.1177/1350650113484097
13. Andersson M, Sosa M, Olofsson U (2016) The effect of running-in on the efficiency of superfinished gears. Tribol Int 93:71–77. https://doi.org/10.1016/j.triboint.2015.08.010
14. Sjöberg S, Sosa M, Andersson M, Olofsson U (2016) Analysis of efficiency of spur ground gears and the influence of running-in. Tribol Int 93:172–181. https://doi.org/10.1016/j.triboint.2015.08.045
15. Sosa M, Sellgren U, Björklund S, Olofsson U (2016) In situ running-in analysis of ground gears. Wear 352-353:122–129. https://doi.org/10.1016/j.wear.2016.01.021
16. Mallipeddi D, Norell M, Sosa M, Nyborg L (2017) Influence of running-in on surface characteristics of efficiency tested ground gears. Tribol Int 115:45–58. https://doi.org/10.1016/j.triboint.2017.05.018
17. Fernandes CMCG, Martins RC, Seabra JHO (2014) Torque loss of type C40 FZG gears lubricated with wind turbine gear oils. Tribol Int 70:83–93. https://doi.org/10.1016/j.triboint.2013.10.003
18. Fernandes CMCG, Marques PMT, Martins RC, Seabra JHO (2015) Gearbox power loss. Part I: losses in rolling bearings. Tribol Int 88:298–308. https://doi.org/10.1016/j.triboint.2014.11.017
19. Mummery L (1990) Surface texture analysis: the handbook. Hommelwerke,
20. Tallian TE (1967) On competing failure modes in rolling contact. A S L E Transactions 10(4):418–439. https://doi.org/10.1080/05698196708972201
21. Dowson D, Higginson GR (1977) Elasto-hydrodynamic lubrication. Pergamon Press, Oxford
22. Archard JF (1953) Contact and rubbing of flat surfaces. J Appl Phys 24(8):981–988. https://doi.org/10.1063/1.1721448
23. Brandão JA, Cerqueira P, Seabra JH, Castro MJ (2016) Measurement of mean wear coefficient during gear tests under various operating conditions. Tribol Int 102:61–69. https://doi.org/10.1016/j.triboint.2016.05.008
24. Fernandes CMCG, Marques PMT, Martins RC, Seabra JHO (2015) Gearbox power loss. Part II: friction losses in gears. Tribol Int 88:309–316. https://doi.org/10.1016/j.triboint.2014.12.004
25. Marques PMT, Fernandes CMCG, Martins RC, Seabra JHO (2014) Efficiency of a gearbox lubricated with wind turbine gear oils. Tribol Int 71:7–16. https://doi.org/10.1016/j.triboint.2013.10.017
26. Fernandes CMCG, Marques PMT, Martins RC, Seabra JHO (2015) Gearbox power loss. Part III: application to a parallel axis and a planetary gearbox. Tribol Int 88:317–326. https://doi.org/10.1016/j.triboint.2015.03.029
27. Fernandes CMCG, Marques PMT, Martins RC, Seabra JHO (2015) Influence of gear loss factor on the power loss prediction. Mech Sci 6(2):81–88. https://doi.org/10.5194/ms-6-81-2015
28. Martins RC, Fernandes CMCG, Seabra JHO (2015) Evaluation of bearing, gears and gearboxes performance with different wind turbine gear oils. Friction 3(4):275–286. https://doi.org/10.1007/s40544-015-0094-2
29. SKF (2003) SKF general catalogue
30. Marshall G, Jonker L (2010) An introduction to descriptive statistics: a review and practical guide. Radiography 16(4):e1–e7. https://doi.org/10.1016/j.radi.2010.01.001
31. Tabachnick BG, Fidell LS (2006) Using multivariate statistics, 5th edn. Allyn & Bacon, Inc, Needham Heights, MA, USA
32. Touret T (2019) Health monitoring: impact thermique d'un default dans une transmission par engrenages – application aeronautique. Université de Lyon, Lyon